Intracellular delivery of oligonucleotides in *Helicobacter pylori* by fusogenic liposomes in the presence of gastric mucus

Rita S. Santos[1,2,3,4], George R. Dakwar[1], Elisa Zagato[1,5], Toon Brans[1,5], Céu Figueiredo[3,4,6], Koen Raemdonck[1], Nuno F. Azevedo[2], Stefaan C. De Smedt[1*] and Kevin Braeckmans[1,5]

[1]Laboratory of General Biochemistry and Physical Pharmacy, Ghent University, Ghent, Belgium;

[2]LEPABE, Department of Chemical Engineering, Faculty of Engineering of the University of Porto, Porto, Portugal;

[3]i3S, Instituto de Investigação e Inovação em Saúde, Universidade do Porto, Porto, Portugal;

[4]IPATIMUP, Institute of Molecular Pathology and Immunology of the University of Porto, Porto, Portugal;

[5]Center for Nano- and Biophotonics, Ghent University, Ghent, Belgium;

[6]Department of Pathology and Oncology, Faculty of Medicine of the University of Porto;

***** Corresponding author. Mailing address: Laboratory of General Biochemistry and Physical Pharmacy, Faculty of Pharmaceutical Sciences, Ghent University, Ottergemsesteenweg 460, 9000 Ghent, Belgium. Phone: 003292648076; Fax: 003292648189. E-mail: Stefaan.DeSmedt@UGent.be

Abstract

The rising antimicrobial resistance contributes to 25000 annual deaths in Europe. This threat to the public health can only be tackled if novel antimicrobials are developed, combined with a

more precise use of the currently available antibiotics through the implementation of fast, specific, diagnostic methods. Nucleic acid mimics (NAMs) that are able to hybridize intracellular bacterial RNA have the potential to become such a new class of antimicrobials and additionally could serve as specific detection probes. However, an essential requirement is that these NAMs should be delivered into the bacterial cytoplasm, which is a particular challenge given the fact that they are charged macromolecules.

We consider these delivery challenges in relation to the gastric pathogen *Helicobacter pylori*, the most frequent chronic infection worldwide. In particular, we evaluate if cationic fusogenic liposomes are suitable carriers to deliver NAMs across the gastric mucus barrier and the bacterial envelope. Our study shows that DOTAP-DOPE liposomes post-PEGylated with DSPE-PEG (DSPE Lpx) can indeed successfully deliver NAMs into *Helicobacter pylori*, while offering protection to the NAMs from binding and inactivation in gastric mucus isolated from pigs. DSPE Lpx thus offer exciting new possibilities for *in vivo* diagnosis and treatment of *Helicobacter pylori* infections.

Keywords: Infections, Lipoplexes, Gastric Mucus, Nucleic Acid Mimics, *Helicobacter pylori*

Introduction

Infectious diseases are responsible for 14 million annual deaths, representing around 90% of the health problems worldwide [1]. Infections that could be treated for decades by classic antibiotics have become a serious threat to human health due to the advent of antimicrobial resistance [1, 2]. However, nucleic acid mimics (NAMs) designed to specifically hybridize *in situ* with complementary bacterial RNA, hold promise both for treatment and diagnosis of infections. Contrary to traditional oligonucleotides, NAMs are composed of modified DNA or

RNA sugars that make them resistant to endonuclease degradation and improve their affinity towards RNA targets [3-6].

NAMs can be designed to act as antisense antimicrobials, by hybridizing and consequently inhibiting the expression of selected genes [7-9]. These can be essential bacterial genes, thus preventing bacteria growth, or genes involved in the resistance to antibiotics, thus restoring bacteria susceptibility to antibiotics. This strategy provides a potentially endless source of active antibacterials. Even if the bacterial target undergoes a point mutation, which is the most common form of resistance to antibiotics [10], the oligonucleotide can be easily redesigned to become effective again.

In addition, NAMs conjugated with a contrast agent could serve as detection probes for rapid and comprehensive *in vivo* diagnosis. They could detect not only the presence of specific bacteria, but also the presence of bacterial genes responsible for resistance to antibiotics, so that an effective antibacterial drug can be prescribed in time [3, 11-14]. Compared to the current diagnostic techniques, labelled NAMs have the potential to overcome the traditional time-consuming culture methods as well as the need of bacteria isolation and extraction of target genetic material associated with other molecular methods, like PCR [2, 12, 15].

In addition to their value for therapy and clinical diagnosis, the opportunity to directly localize bacteria *in vivo* is also of interest for research purposes. The host-microbial and microbial-microbial interactions, which can have an impact on the immune system and disease state, are mostly missed by the lack of a technique to visualize live bacteria within their *in vivo* environment [13, 16, 17]. NAMs hold the potential to respond to this need.

For NAMs to fulfil their promise as a flexible platform for diagnosis and treatment of bacterial infections, they should be safely delivered across biological barriers in the body. Mucus in the gastrointestinal, respiratory, reproductive and urinary tracts presents a first barrier for NAMs [18-20]. Mucus is a highly complex and viscoelastic network able to bind foreign

entities (through electrostatic, hydrophobic or hydrogen bonds) and/or sterically obstruct particles which are larger than the size of the pores in mucus [19, 21, 22]. Therefore, NAMs need to be able to pass through mucus to reach the target bacteria [23]. Importantly, they should do so without losing their activity. Indeed, we have recently shown that interactions with gastric mucus can significantly compromise the ability of NAMs to hybridize with *Helicobacter pylori* (*H. pylori)* [24].

Apart from crossing the mucus layer, it is pivotal that the NAMs are delivered into the cytoplasm of bacterial cells. Unlike eukaryotic cells, bacteria possess a multi-layered cell envelope which is recognized as a challenging barrier for oligonucleotide penetration [8, 25]. Strategies to permeabilize the bacterial envelope *in vitro* include electroporation, enzymatic (e.g. lysozyme) or chemical (e.g. ethanol) treatment. None of those are, however, easily transferable to *in vivo*. While cell-penetrating peptides (CPPs) conjugated to antisense NAMs may be promising [14, 26-30], conventional CPPs induce cytotoxicity and possess low *in vivo* stability [31-34]. In addition, bacterial resistance to CPP-mediated penetration has been reported [32].

In this work we have considered both delivery challenges, i.e. crossing mucus and the cell envelope, in the context of gastric *H. pylori* infection (Figure 1a), which is the most frequently occurring chronic bacterial infection worldwide [35]. *H. pylori* reside within the gastric mucus layer as well as in close proximity with the epithelial cells underlying the gastric mucus layer [36]. Here we investigated if fusogenic stealth liposomes are suitable nanocarriers for NAMs to target *H. pylori* infections. Liposomes have been extensively studied to deliver nucleic acids into eukaryotic cells [37]. Until now their application to treat bacterial infections is almost exclusively limited to the delivery of traditional small molecule antibiotics [38-41]. So far, only two papers report on the use of liposomes to deliver phosphorothioate DNA in *Escherichia coli*

and in *Staphylococcus aureus* [42, 43]. In spite of its promise it shows that liposomal delivery of nucleic acids into bacteria is a virtually unexplored area.

In the current study we use fusogenic cationic liposomes, made from the lipids DOTAP and DOPE, which are well-characterized carriers for nucleic acids in eukaryotic cells [44-46]. We reasoned that DOTAP-DOPE liposomes may be of interest for delivery in gram negative bacteria due to the presence of the fusogenic lipid DOPE which may promote fusion of the liposomes with the cell envelope, thus delivering its content into the cell's cytoplasm [47, 48]. Based on our previous work, locked nucleic acids (LNA) and 2'-OMethyl RNA (2'OMe), with either phosphodiester (PO) or phosphorothioate (PS) as backbone linkages (Figure 1b), were used as NAMs to hybridize to *H. pylori* rRNA [24, 49]. Electrostatic complexes between (anionic) NAMs and (cationic) DOTAP-DOPE liposomes were formed, which were further modified by post-insertion of PEG-lipids with the aim to improve the stability and mobility of the complexes in the harsh gastrointestinal environment [50, 51]. We tested two PEGylation strategies: DSPE-PEG that stably incorporates into liposomes and Cer-PEG that can diffuse out of the liposomes over time [52, 53]. First, we evaluated if those PEGylated lipoplexes have good diffusional mobility in gastric mucus isolated from pigs, being a clear prerequisite to be able to reach the bacteria dispersed in the mucus. Next, it was investigated whether the PEGylated lipoplexes could deliver NAMs into *H. pylori* in suspension by fluorescence *in situ* hybridization (FISH). Finally, we assessed if the PEGylated lipoplexes could still successfully deliver functional NAMs in *H. pylori* in the presence of gastric mucus.

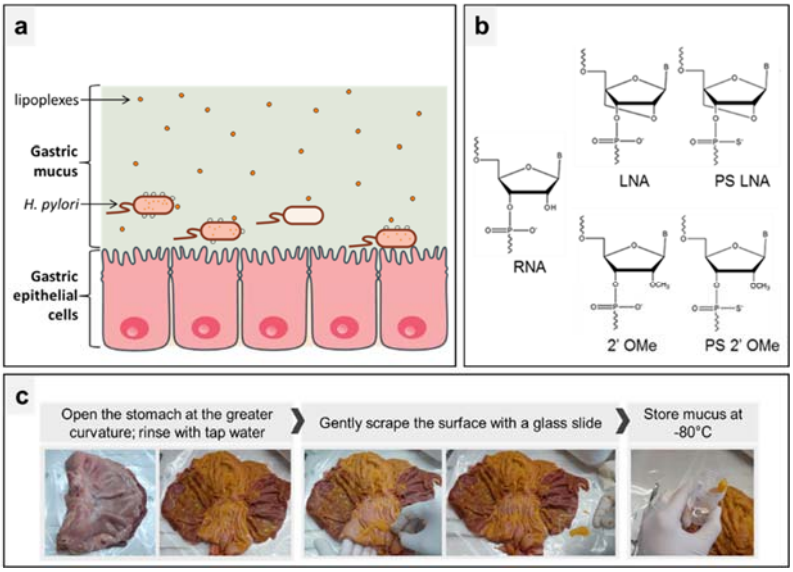

Figure 1. (a) Illustration of the study concept: representation of liposomal delivery of NAMs across the gastric mucus to target *H. pylori*. (b) Monomers of the NAMs used in FISH, compared to RNA. (c) Procedure followed for the collection of mucus from the stomach of pigs. (Adapted from [24] and [49]).

Materials and Methods

Materials

(2,3-Dioleoyloxy-propyl)-trimethylammonium-chloride (DOTAP), 1,2-dioleoyl-sn-glycero-3-phosphoethanolamine (DOPE), 1,2-Distearoyl-sn-glycero-3-phosphoethanolamine-N-(methoxy(polyethyleneglycol)-2000) (DSPE-PEG), N-octanoyl-sphingosine-1-succinyl[methoxy(polyethylene glycol)2000] (CerC8-PEG) and DOPE-LissamineRhodamineB were purchased from Avanti Polar Lipids (Alabaster, AL). Yellow-green (505/515) fluorescent carboxylate-modified polystyrene FluoSpheres® of 40, 100, 200 and 500 nm of diameter were purchased from Invitrogen Molecular Probes (Eugene, OR). N-(3-Dimethylaminopropyl)-N′-ethylcarbodiimide hydrochloride (EDC) and N-

Hydroxysulfosuccinimide sodium salt (sulfo-NHS) were acquired from Sigma-Aldrich (Bornem, Belgium) and 2 kDa methoxy-polyethylene glycol-amine (mPEGa) from Creative PEGWorks (Winston Salem, USA). Chloroform, 4-(2-hydroxyethyl)-1-piperazineethanesulfonic acid (HEPES), 2-Amino-2-(hydroxymethyl)-1,3-propanediol hydrochloride (Tris-HCl), sodium chloride (NACl) and triton X-100 were purchased from Sigma-Aldrich (Bornem, Belgium). Paraformaldehyde was acquired from Fluka – Sigma-Aldrich, (Bornem, Belgium). Urea was purchased from Vel – VWR (Haasrode, Belgium). Pepsin (from porcine gastric mucosa) was purchased from Merck Millipore (Madrid, Spain). Trypticase soy agar plates supplemented with 2% (v/v) sheep blood were purchased from Becton Dickinson GmbH (Erembodegem, Belgium). CampyGen sachets to generate microaerobic conditions were acquired from Oxoid – Thermo Scientific (Waltham, MA, USA).

Collection of porcine gastric mucus

Mucus scraped from the stomach of pigs was used in this study, as its bio-relevance is markedly higher than mucus solutions prepared from commercial mucins [54, 55]. Also, pigs have a gastric physiology similar to humans, making them representative animal models for *Helicobacter* infection studies [56, 57].

Stomachs were collected from a local slaughterhouse, opened at the greater curvature and gently rinsed with tap water to remove most of the food debris [58]. The mucus, loosely bound and adherent, was then gently scrapped off with a glass slide, aliquoted and stored at -80°C. Mucus from three different pigs was included in each experiment.

NAMs synthesis

Two oligonucleotides complementary to a sequence of the *H. pylori* 16S rRNA gene, were used in this study. These are composed of LNA and 2'OMe, possess the same sequence and

differ only in the internucleotide bonds. One possesses normal phosphodiester oligonucleotides (PO), while the other has one of the two non-bridging oxygen atoms replaced by a sulphur atom at each internucleotide linkage (PS) (Figure 1b). These oligonucleotides will be herein designated as PO and PS, respectively. The sequence of PO is 5'-lGmeAmeClTmeAmeAlGmeCmeClC-3', while the sequence of PS is 5'-lG*meA*meC*lT*meA*meA*lG*meC*meC*lC*-3', where "l" represents the LNA monomers, "me" the 2'OMe monomers and * the phosphorothioate linkages. These oligonucleotides were fluorescently labelled at 5' with Cy3. They were synthetized and purified according to [49].

Preparation of liposomes and lipoplexes and colloidal stability in simulated gastric juice

Cationic liposomes composed of DOTAP and DOPE (in a 1:1 molar ratio) were prepared as reported before [59]. In brief, the lipids dissolved in chloroform were mixed and a dry lipid film was prepared by rotary evaporation of the chloroform at 40 ºC. The lipid film was hydrated with 20 mM HEPES buffer (pH 7.2) and sonicated using a probe sonicator (Branson Ultrasonics Digital Sonifier®, Danbury, USA), resulting in a final concentration of 5 mM DOTAP and 5 mM DOPE. The average hydrodynamic size and zeta potential of the cationic liposomes was routinely checked by dynamic light scattering (Zetasizer Nano-ZS, Malvern, Worcestershire, UK).

Lipoplexes were prepared through complexation of cationic liposomes with Cy3 labeled NAMs at a +/- charge ratio of 15; the +/- charge ratio is calculated as the molar amount of positive charges on the DOTAP molecules, divided by the molar amount of negative charges on the NAMs (with 1 NAM molecule containing 10 negatively charged phosphate groups).

Complexation was performed by addition of a diluted dispersion of cationic liposomes to a NAM-solution (PS or PO), followed by incubation for 30 min, at room temperature.

PEGylation of the thus obtained lipoplexes was performed by 'post-insertion' of PEG lipids (2kDa CerC8-PEG or 2kDa DSPE-PEG) [60]. Therefore, the PEG lipids were first re-dissolved in sterile milli-Q water (after chloroform removal by nitrogen flush), added to the DOTAP-DOPE-NAM complexes and incubated for 1h at 37 ºC. The PEG lipids accounted for 10% of the total lipids in the lipoplexes. The post-PEGylation efficacy was evaluated from the decrease in the (absolute) zeta potential value of the complexes, measured with the Zetasizer Nano-ZS. Throughout the paper, cationic lipoplexes are referred as Lpx, lipoplexes post-PEGylated with DSPE-PEG as DSPE Lpx, and lipoplexes post-PEGylated with Cer-PEG as Cer Lpx.

Upon oral intake, the formulations will come in contact with the gastric juice. Therefore, we first tested if the liposomes are colloidally stable in simulated gastric juice (sGJ). The sGJ was prepared according to the US pharmacopeia: a solution of 0.2% (w/v) NaCl, 0.32% (w/v) gastric pepsin and 0.7% (v/v) HCl, final pH ≈ 1.2. The liposomes were diluted (10 times) in sGJ and incubated during 4 hours at 37 ˚C. Their hydrodynamic diameter was measured by dynamic light scattering.

PEGylation of polystyrene nanospheres

To assess the effect of the size of nanoparticles on their diffusion through gastric mucus isolated from pigs, polystyrene FluoSpheres® were PEGylated to render them muco-inert. Indeed, PEGylation may avoid the potential binding of the nanospheres to compounds present in mucus [20, 22].

Yellow-green (505/515) fluorescent carboxylate-modified polystyrene FluoSpheres® of 40, 100, 200 and 500 nm nominal diameter were covalently modified with PEG via amine coupling, as described elsewhere [50, 61]. In brief, mPEGa, EDC and sulfo-NHS were dissolved in

HEPES Buffered Saline (HBS, pH 8). The nanospheres were added to this mixture so that a final concentration of 4 mg/mL EDC, 1.13 mg/mL sulfo-NHS, 10 mg/mL mPEGa and 1% solids (nanospheres) was obtained. The reaction mixture was left shaking overnight, at 200 rpm. Purification was then performed using a centrifugal filter (Amikon ultra centrifugal filters, 100 K membrane, Millipore, MA, USA) for 12 min at 14,000 rpm, followed by two washings in HBS (12 min at 14,000 rpm). The filter was then placed upside down in a new vial and the purified PEGylated nanospheres were collected after centrifugation for 3 min at 1,000 rpm. They were resuspended in HBS to a final concentration of 2% solids (nanospheres) and stored at 4°C, until use. To allow optimal PEG coverage a slightly different protocol was used for the polystyrene nanospheres of 40 nm nominal diameter. The reaction mixture contained 0.5% solids (40 nm nanospheres) and it was left rotating for 5 days, at 30 rpm, using a Hulamixer (Life Technologies, Carlsbad, CA, USA). Purification was done by dialysis for 6h, employing a Slide-A-Lyzer™ dialysis cassette with a 10 kDa molecular weight cut off (Thermo Scientific, Waltham, MA, USA), followed by ultracentrifugation (L8-70 M, Beckman, Coulter, Fullerton, CA, USA). The purified PEGylated 40 nm nanospheres were resuspended in HBS to a final concentration of 1% solids and stored at 4 °C.

PEGylation of the polystyrene nanospheres was confirmed by measuring the zeta potential of the nanospheres in HEPES buffer, before and after reaction, using a Zetasizer Nano-ZS.

Diffusion measurements of polystyrene nanospheres and lipoplexes in gastric mucus by single particle tracking (SPT)

Diffusion measurements on the PEGylated polystyrene nanospheres and the (fluorescent) lipoplexes in mucus from the stomach of pigs were performed by fluorescence single particle tracking (SPT), at 37 °C, as described by our group elsewhere [50, 62]. For this, the PEGylated nanospheres were first sonicated for 5 min and diluted in sterile milli-Q water to a concentration suitable for SPT-measurements. Five μL of the diluted PEGylated nanospheres was gently

mixed with ≈ 30 μL of mucus (taken with a plastic syringe, due to its high viscosity). This mixture was placed between a microscope slide and a coverslip with a double-sided silicon spacer of 1 mm thickness and 20 mm diameter in between (Press-to-seal silicone isolators; Molecular Probes, Leiden, The Netherlands). Measurements in sterile milli-Q water were performed as a control. For these, 7 μL of properly diluted PEGylated nanospheres was placed between a microscope slide and a coverslip with a double-sided adhesive spacer of 0.12 mm thickness and 9 mm diameter in between (Secure-Seal spacer; Molecular Probes, Leiden, The Netherlands). Before starting the SPT-measurements, the samples were equilibrated for 10 min at 37 °C in a stage-top incubator (Tokai Hit, Fujinomiya, Japan) mounted on the microscope.

The diffusion measurements on the lipoplexes (Lpx, Cer Lpx and DSPE Lpx) were performed in the same way as described above for the PEGylated nanospheres. For these measurements, the liposomes were prepared to contain 1 mol% DOPE-LissamineRhodamineB for fluorescence imaging within the mucus.

To study the diffusion of the fluorescent nanospheres and lipoplexes, typically 25 to 35 'SPT-movies' were recorded at different locations in the mucus. Each SPT-movie was 5 s long and consisted of about 155 frames (recorded at a rate of 30.9 frames per second). The SPT-measurements were done on a custom-built laser wide field microscope setup [50, 62]. The videos were analysed using an in-house developed software [63] to translate the nanoparticles trajectories into a distribution of apparent diffusion coefficients.

Fluorescence *in situ* hybridization in *H. pylori* in suspension by free NAMs and lipoplexes

H. pylori 26695 (ATCC 700392) was grown in trypticase soy agar supplemented with 5% sheep blood (Becton Dickinson GmbH, Germany) for 48 hours, at 37 °C, under microaerobic conditions. The bacteria were then harvested from the agar plates, using sterile saline solution,

and diluted to nearly $2x10^8$ cells/mL. The FISH procedure was based on a previously reported protocol [64], with some modifications. The bacteria in suspension were either treated with ethanol or mixed directly with the lipoplexes.

For FISH experiments by ethanol based permeabilization of the bacteria, 100 µL of the bacterial suspension was pelleted by centrifugation for 15 min at 10,000 x g and resuspended in 500 µL of 50% (v/v) ethanol, for 15 min. Large *H. pylori* aggregates were removed by filtration through a sterile 10 µm pore size filter (CellTrics®, Görliz, Germany). 100 µL of the ethanol treated bacteria was then resuspended in 100 µL of hybridization solution (900 mM NaCl, 500 mM Urea, 50 mM Tris-HCl, pH 7) containing 400 nM of Cy3 labelled NAM PS or PO.

For FISH experiments using lipoplexes, 100 µL of the initial bacterial suspension (diluted to a similar concentration as described above for the ethanol treatment) was resuspended in 100 µL of hybridization solution containing lipoplexes (Lpx, Cer Lpx or DSPE Lpx) instead of free NAM. The amount of lipoplexes added was such that 400 nM of NAM PS or PO was present in the hybridization mixture. To be able to take into account the auto-fluorescence of *H. pylori,* negative control experiments were performed on bacteria resuspended in hybridization solution without NAM, for the conditions tested (with/without ethanol permeabilization and liposomes). As all negative controls looked the same, we only present example images of bacteria without exposure to ethanol nor liposomes. Hybridization was then performed by incubating the sample at 37 °C, for 30 min. Hybridization was followed by a washing step. For this, the bacteria were pelleted by centrifugation at 10,000 x g for 5 min, and resuspended in 500 µL of pre-warmed (37 °C) aqueous solution at pH 7. Instead, some samples were resuspended in 500 µL of a 0.1% (v/v) Triton X-100 solution to remove lipoplexes that remain bound to the bacterial outer membrane. The samples were then incubated at 37 °C, for 15 min. After washing, the bacteria were centrifuged at 10,000 x g for 5 min and resuspended in sterile milli-Q water. 20 µL of

bacterial suspension was placed on a diagnostic slide (Thermo Scientific, Waltham, MA, USA) and allowed to dry at 37 °C.

The slides were mounted with immersion oil and a coverslip and visualised under the microscope. Microscopy images were acquired using a Nikon TE2000 microscope equipped with a Nikon DS-Qi 1Mc digital camera and a Plan Apo VC 100× 1.4 NA oil immersion objective lens (Nikon). Cy3 fluorescence was visualized using a TRITC filter (excitation: 530-560 nm; emission: 590-650 nm, Nikon). For fluorescence quantification, all samples were analysed using the same exposure time and the same excitation intensity; around 10 images per slide well were taken at different locations of the well.

Fluorescence *in situ* hybridization in *H. pylori* by free NAMs and DSPE Lpx exposed to gastric mucus

The hybridization efficiency of free NAMs and DSPE Lpx (being the Lpx which transfected *H. pylori* in suspension the most successfully, see above), mixed with porcine gastric mucus was subsequently tested. As this required the application of mucus on top of the bacteria, it was not feasible to perform FISH on bacteria in suspension; instead FISH was performed on bacteria applied on glass slides, following the method we reported before [24]. Briefly, *H. pylori* in the exponential growth phase was harvested from the agar plates, using sterile saline solution, and diluted to nearly $1.6x10^6$ cells/mL. Smears were prepared on glass slides (20 µL per slide well) by drying at 37 °C. To avoid cytotoxic effects of porcine mucus, as reported by others [65], the bacterial cells were fixed before contact with the mucus by incubation with 40 µL of 4% (w/v) paraformaldehyde, for 10 min. The free NAMs or the DSPE Lpx were 10x diluted in hybridization solution. 20 µL of these samples was added to approximately 30 µL of mucus and gently mixed. The final concentration of NAMs (whether free or in lipoplexes) within this mucus mixture was 400 nM (as is the case in the FISH experiments described above on FISH

in suspension). The bacteria smear on the glass slide was covered by the mucus mixture and closed by a coverslip. The slide was placed in a dark moist chamber, hybridization was allowed for 30 min, at 37 °C. After hybridization the coverslip was removed together with the mucus mixture and the slide was washed during 15 min, 37 °C, in pre-warmed aqueous solution, at pH 7. The slide was allowed to dry and fluorescence quantification was done as described above. To be able to take into account the auto-fluorescence of *H. pylori*, negative controls were performed using hybridization solution without free NAMs nor lipoplexes.

Quantification of *H. pylori* hybridization

For both hybridization with and without mucus the quantification was based on fluorescence microscopy and image processing, so that a reliable comparison could be done between all conditions; flow cytometry quantification would not be an option since it is not applicable to hybridization with mucus.

The fluorescence of the bacteria obtained in the FISH experiments was quantified using an in-house developed software based on image processing routines available in Matlab (The MathWorks, Natick, MA, USA). First, bacteria were identified in each image based on an automatically determined intensity threshold. This results in a binary mask that corresponds to the location of bacteria in the image. For the regions within the mask, the average fluorescence intensity in the original image (F_{image}) was quantified as:

$$F_{image} = \frac{\sum_{b=1}^{n}[(f_b - BG_b) \times \#pix_b]}{\sum_{b=1}^{n} \#pix_b},$$

where b refers to each bacterium, n corresponds to the number of bacteria in the image, f_b corresponds to the mean pixel fluorescence of each bacterium, BG_b is the local background value around each bacterium and $\#pix_b$ is the number of pixels comprising each bacterium.

Per sample, around 10 images were analysed in this fashion. Three repeated samples were analysed per treatment, from which the average fluorescence intensity was calculated. These

absolute values were normalized to the respective positive control of PS or PO. Three independent experiments were performed and the average normalized fluorescence from the 3 treatment replicates was finally obtained.

Statistical analysis

Statistical analysis was performed by GraphPad Prism6 software (GraphPad Software, San Diego, USA). The FISH results were analysed using two-way analysis of variance (ANOVA) and Sidak's multiple comparison test, comparing the samples with the respective reference (fluorescence 1) within the same NAM. Fluorescence 1 corresponds to ETH+NAM (Figure 3 and 5), or NAM (Figure 6). Significance was set at $P \leq 0.05$ (**** $P \leq 0.0001$, *** $P \leq 0.001$, ** $P \leq 0.01$, * $P \leq 0.05$).

Results

Characterization of the liposomes and lipoplexes

Cationic liposomes were prepared from DOTAP and DOPE, in a 1:1 molar ratio, following the lipid film hydration method [59]. The liposomes had an average hydrodynamic diameter of around 80-100 nm and an average zeta potential about +40-55 mV. Cationic lipoplexes were prepared by incubation of DOTAP-DOPE liposomes with NAM PS or PO. The cationic lipoplexes (Lpx) were subsequently post-PEGylated with Cer-PEG (Cer Lpx) or DSPE-PEG (DSPE Lpx). Both types of PEG chains were successfully inserted into the complexes, as was observed from the decrease in zeta potential of the lipoplexes (Figure S1a). In all cases the final zeta potential of the PEGylated lipoplexes was around 15 mV, with an average hydrodynamic diameter ranging from 98 nm to 133 nm (Figure S1a). Upon oral intake, liposomes will come into contact with the gastric juice. We, therefore, tested the colloidal stability of the liposomes

(both for non-PEGylated and PEGylated liposomes) in simulated gastric juice, and found that their size remains constant for at least 4h (Figure S2a). Together with the chemical stability of free NAMs under gastric pH [64], it is a strong indication that the gastric juice will not impose a constraint in a clinical application.

Diffusion measurements of polystyrene nanospheres and lipoplexes in gastric mucus by single particle tracking (SPT)

As gastric mucus represents a challenging diffusional barrier, we first evaluated how the size of nanoparticles influences their mobility in gastric mucus. To that end, the diffusion of model nanospheres of defined sizes was assessed. We noticed that the nanospheres of 40 nm nominal size were actually bigger with a hydrodynamic radius of approximately 60 nm, as measured by dynamic light scattering (Figure S1b); therefore, in our results we refer to them as ’60 nm’ nanospheres (instead of ’40 nm’). The nanospheres were first PEGylated to avoid muco-adhesion [21, 50]. The PEG could be conjugated to the polystyrene nanospheres, as judged from the clear zeta potential change towards neutral values (Figure S1b).

As expected, due to the size-filtering effect of mucus [19], the larger the PEGylated nanospheres, the lower their diffusional mobility in gastric mucus, as measured by SPT (Figure 2a and Table S1; example movies 1-4 in supplementary material). Both 60 and 100 nm nanospheres showed a bimodal distribution of diffusion coefficients, indicating that a part of those particles is mobile while another fraction is immobilized. The mobile fraction was clearly smaller for the 200 nm nanospheres and almost non-existing for the 500 nm particles. This shows that the mesh size of gastric mucus is quite heterogeneous, as already observed before for gastrointestinal mucus [18, 19]. Other types of mucus do not seem to show such high level of heterogenicity; for instance in cystic fibrosis sputum PEGylated nanospheres of 100 nm and 200 nm (similar to the ones used here) showed good and uniform mobility with an unimodal

388 distribution of diffusion coefficients [50]. Our diffusion results in gastric mucus indicate that
389 nanoparticles should preferably be as small as possible for efficient diffusion in gastric mucus,
390 and in any case they should be smaller than 200 nm.

391 While the lipoplexes under investigation do fulfil this criterion, their diffusion in porcine
392 gastric mucus was experimentally verified by SPT as well (example PS movies 5-7 in mucus
393 and movies 8-10 in water in supplementary material). Figure 2b show that non-PEGylated Lpx
394 (Lpx) clearly had the lowest mobility, as could be expected due to interactions with mucus
395 constituents. Post-PEGylation (Cer Lpx and DSPE Lpx) increases the mobile fraction slightly,
396 resulting in a 3 to 5-fold higher average diffusion coefficient (Table S1). Nevertheless, the
397 improvement of the diffusion by PEGylation is rather moderate and a substantial non-mobile
398 fraction remains present. It confirms that nanoparticle size poses a serious limitation to diffusion
399 in the dense gastric mucus.

400 In our previous study it was found that the type of internucleotide linkage (PS or PO) affected
401 the diffusion and interaction with mucus [24]. In particular, the PS modification (generally used
402 to increase oligonucleotides stability against nucleases and affinity towards the target sequence
403 [66]) led to slower diffusion and increased interaction with mucus components. The current
404 results show that the use of liposomes as carriers for the NAMs removes these differences as
405 they diffuse at a similar rate irrespective of the type of NAM used.

406

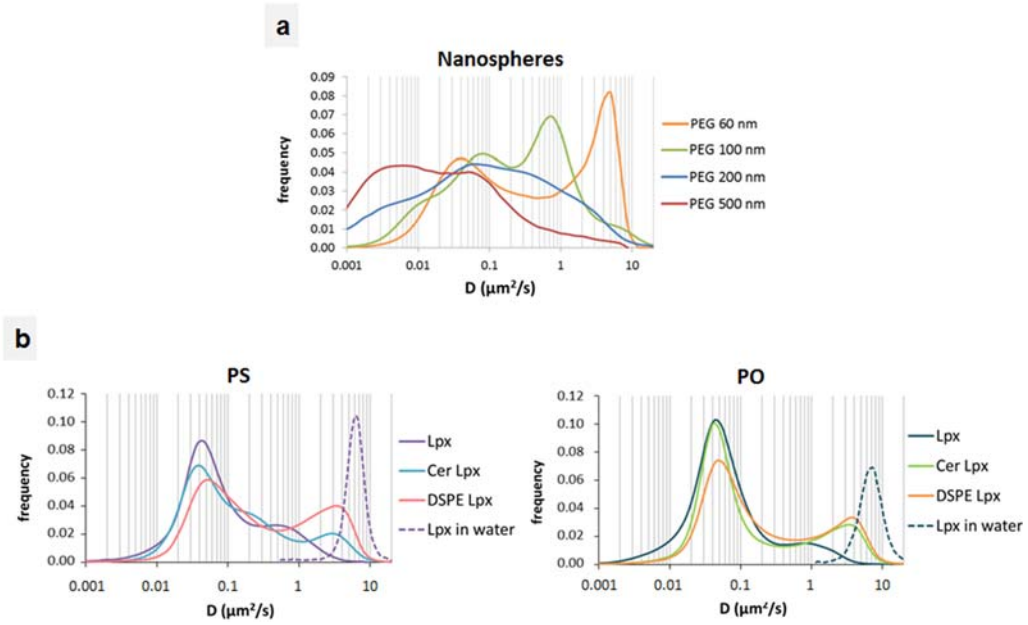

Figure 2. Distribution of diffusion coefficients of polystyrene nanospheres and lipoplexes in gastric mucus isolated from pigs. Results obtained on gastric mucus from 3 different porcine mucus samples were pooled. (a) PEGylated nanospheres of around 60 nm (PEG 60 nm), 100 nm (PEG 100 nm), 200 nm (PEG 200 nm) and 500 nm (PEG 500 nm) in diameter. (b) Cationic lipoplexes (Lpx) compared with Cer Lpx and DSPE Lpx. The dotted line shows the diffusion of Lpx in water.

Fluorescence *in situ* hybridization in *H. pylori* in suspension by free NAMs and lipoplexes

After crossing the gastric mucus, lipoplexes should be able to deliver the NAMs across the cell envelope (Figure 1a). To test this, we first compared the hybridization efficiency of lipoplexes in a suspension of *H. pylori* to the 'standard procedure' involving ethanol mediated membrane permeabilization [64]. As presented in Figure 3, similar results were found for PO and PS NAMs. Free NAMs are only slightly taken up by untreated cells, which increases 2-3 fold upon permeabilization of the bacteria with ethanol. Interestingly, Lpx and Cer Lpx performed equally well as the standard ethanol treatment. The lipoplexes functionalized with

DSPE-PEG performed even better, with a 4-fold higher hybridization efficiency as compared to ethanol treatment. Based on our transfection experience with eukaryotic cells it was rather unexpected that non-PEGylated Lpx did not have the best performance, since PEGylation typically reduces the interactions with the cell membrane [67, 68]. We reckon that this is due to the extensive aggregation of non-PEGylated Lpx in the hybridization solution (Figure S2b), which likely reduces the liposomal interaction with the bacterial envelope. PEGylated Lpx, on the other hand, showed excellent colloidal stability in the hybridization solution (Figure S2b). This improved stability did not prevent effective lipoplexes interactions with *H. pylori* membrane (as shown in Figure 3). This is in line with previous reports on antimicrobials delivery into bacteria by PEGylated liposomes [69, 70] which were shown to interact with bacterial cell membranes [71].

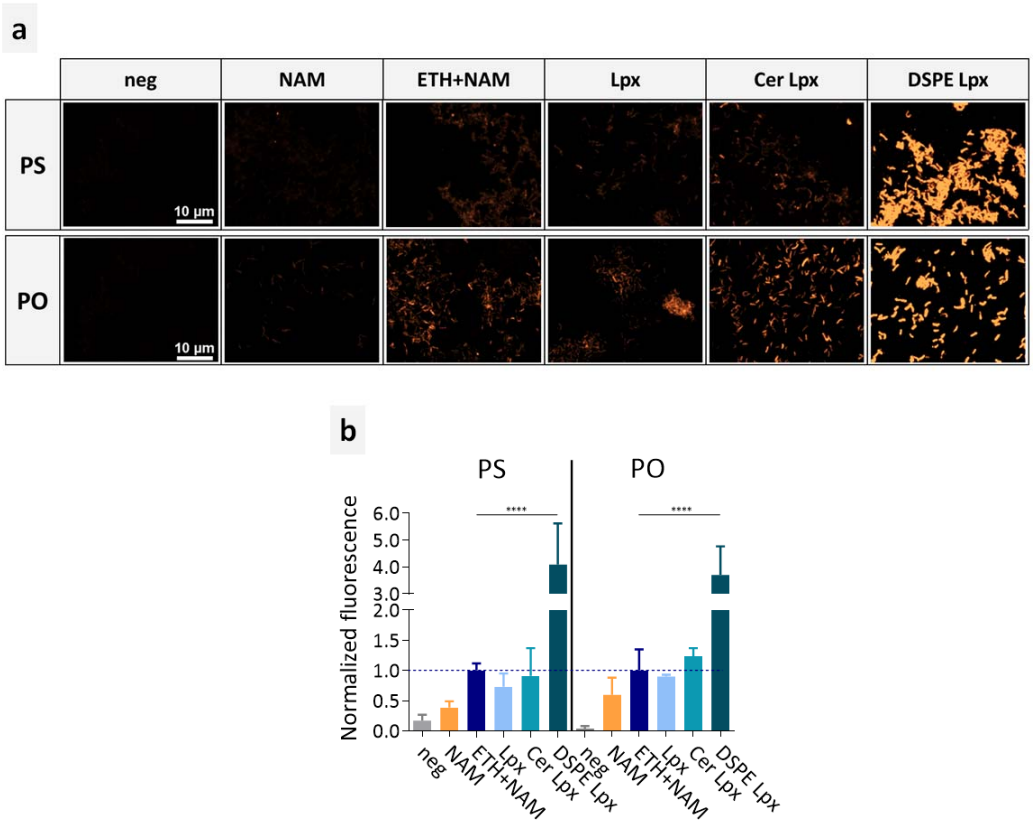

Figure 3. FISH in *H. pylori* in suspension. The hybridization efficiency of Lpx, Cer Lpx and DSPE Lpx was compared with the hybridization efficiencies observed with free NAMs in *H. pylori* respectively not treated (NAM) and pre-treated with ethanol (ETH+NAM), for both PS

and PO. Negative controls without NAM (neg) were also included. (a) Representative epifluorescence microscopy images, all taken with the same exposure time. (b) FISH fluorescence normalized to that of free NAM in ethanol permeabilized *H. pylori* (ETH+NAM). Within one experiment, each condition was performed in triplicate. Three independent experiments were performed. Results are presented as mean values and respective standard deviation.

Confirmation of the intracellular delivery of NAMs in *H. pylori* by DSPE Lpx

The FISH results as presented in Figure 3 are obtained by fluorescence microscopy. It is to be noted, however, that the width of the bacteria is only 0.5-1 µm, which is rather close to the optical resolution limit (~ 0.25 µm). As such, we wanted to confirm that the fluorescence of the bacteria is coming from intracellular NAMs and not just from DSPE Lpx that remain attached to the outer surface of the bacteria. To this end, DSPE Lpx were applied to *H. salomonis*, a morphologically similar *Helicobacter* to which the NAMs should not hybridize [49, 64]. Interestingly, for both PS and PO, DSPE Lpx appeared as fluorescent halos around *H. salomonis* cells, with no fluorescence in the cytosol (Figure 4). This is in stark contrast with the uniform fluorescence that is observed throughout the *H. pylori* cells (Figure 4). This confirms that the observed fluorescence in *H. pylori* at least in part stems from intracellular NAMs retained by hybridization with the target rRNA.

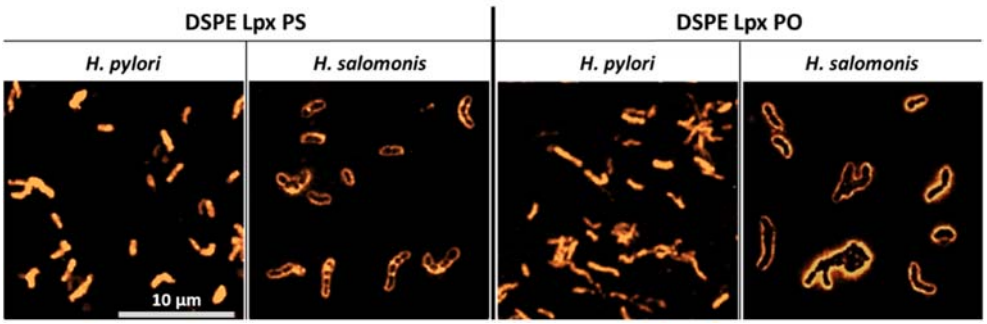

Figure 4. FISH using DSPE Lpx PS and DSPE Lpx PO, respectively, in *H. pylori* and *H. salomonis*. Uniform fluorescence is seen in *H. pylori*, while *H. salomonis* shows a hollow interior with an extracellular fluorescent halo.

It cannot be excluded, however, that part of the observed fluorescence in *H. pylori* results from remaining membrane-bound DSPE Lpx. To find this out, a mild triton wash was performed after hybridization. The samples were washed with a 0.1% (v/v) Triton X-100 solution (instead of the regular washing solution), to remove any remaining lipoplexes that are bound to the outer bacterial membrane. As expected, the extracellular fluorescent halos in *H. salomonis* could be almost completely removed by the triton wash (Figure S3), which demonstrates that this protocol works as intended. When applied to *H. pylori*, the triton did lower the observed fluorescence intensity, leaving only the fluorescence coming from the intracellular NAMs (Figure 5). For PS NAMs, the remaining fluorescence was at the same level as for ethanol permeabilized cells treated with free NAMs. For PO NAMs, the fluorescence remained about 3-fold higher. The reason for this difference is not clear. In conclusion, although a part of the DSPE Lpx PS fluorescence in *H. pylori* did come from membrane bound lipoplexes, these results give clear evidence that NAMs were successfully delivered inside *H. pylori* to an extent that is at least as good as the standard *in vitro* ethanol permeabilization method.

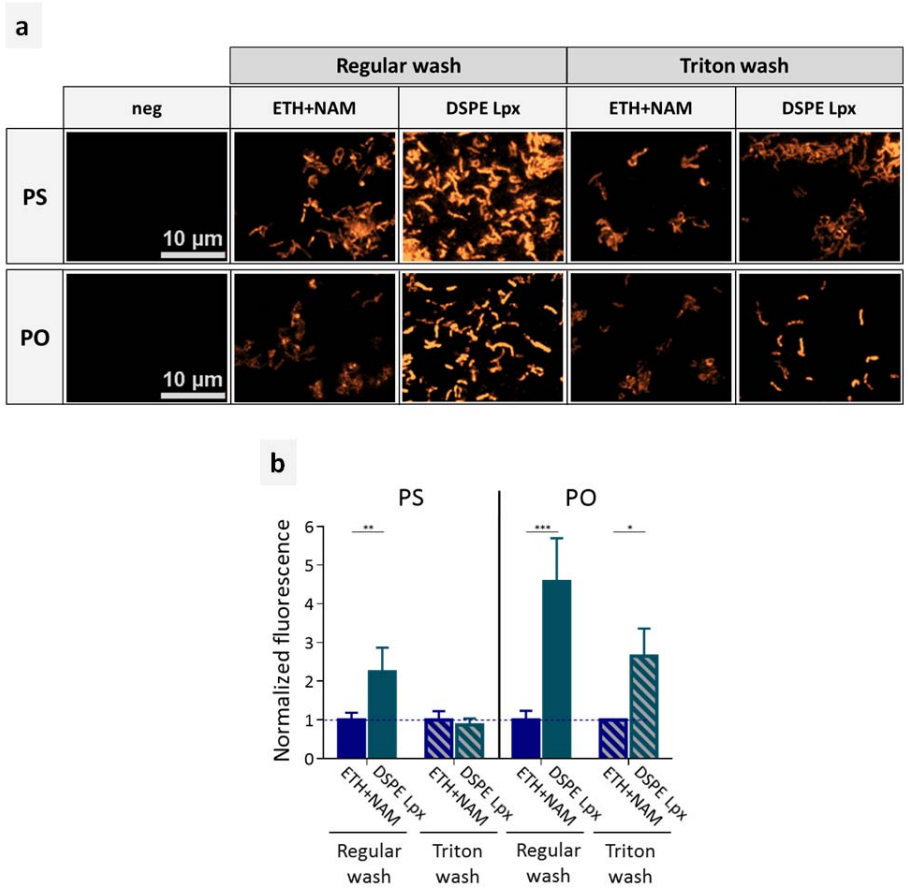

Figure 5. Discrimination between extracellular adhesion and intracellular delivery of NAMs into *H. pylori* cells by lipoplexes. The *H. pylori* fluorescence obtained upon regular wash (representing the total, i.e. intra- plus extracellular, fluorescence) was compared with the one obtained upon mild triton wash (representing the intracellular fluorescence). DSPE Lpx were compared with free NAMs in ethanol treated bacteria (ETH+NAM). Negative controls without NAMs (neg) were also included. (a) Representative epifluorescence microscopy images (all taken with the same exposure time). (b) FISH fluorescence normalized to that of free NAMs in ethanol treated (ETH+NAM) *H. pylori*. Within one experiment, each condition was performed in triplicate. Three independent experiments were performed. Results are presented as mean values and respective standard deviation.

Fluorescence *in situ* hybridization in *H. pylori* by free NAMs and DSPE Lpx exposed to gastric mucus

We showed above that DSPE Lpx can successfully deliver NAMs in *H. pylori* in suspension (Figure 4 and 5) while at least a fraction of DSPE Lpx is mobile in gastric mucus isolated from pigs (Figure 2b). In a next step, we investigated whether hybridization in *H. pylori* by DSPE Lpx is still successful in the presence of gastric mucus. To this end, free NAMs or DSPE Lpx dispersed in hybridization solution were mixed with porcine gastric mucus (in a 2:3 ratio) and applied on top of an *H. pylori* bacterial smear on a glass slide. After incubation for 30 min, the mucus mixture was removed, the slide was washed (regular wash) and cells were imaged by fluorescence microscopy. Compared to free NAMs, the DSPE Lpx show a 2-2.7 fold increase in fluorescence intensity of *H. pylori*, both for PO and PS NAMs (Figure 6). The question again comes if perhaps part of this fluorescence is coming from membrane bound lipoplexes. When the same experiments were performed with *H. salomonis*, the outer fluorescent rim, as observed in solution, was no longer present (Figure S4). This suggests that excessive sticking of lipoplexes to the outer cell envelope does not happen in the presence of mucus, so that the observed fluorescence in *H. pylori* (Figure 6a and 6b) can be ascribed to intracellularly delivered and hybridized NAMs. Taken together we conclude that DSPE Lpx (both PS and PO) have the capacity to deliver NAMs into *H. pylori* even in the presence of the tough gastric mucus barrier.

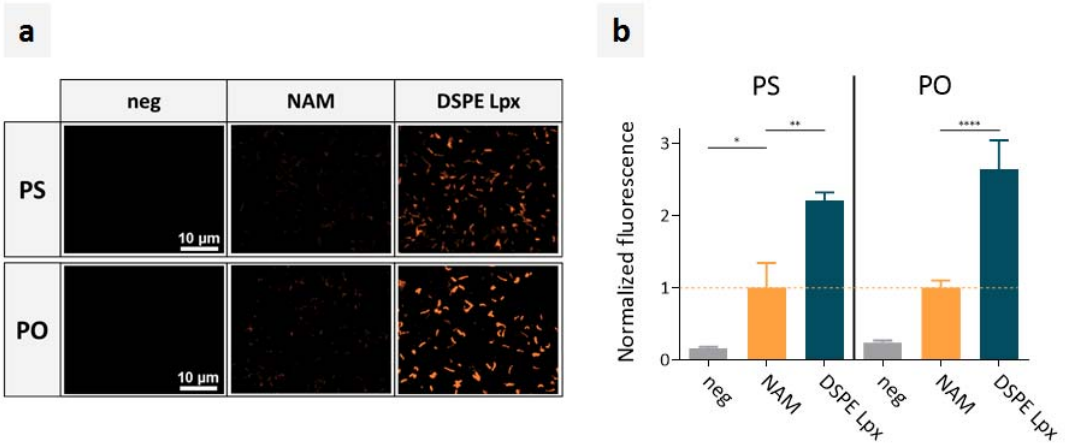

Figure 6. FISH in *H. pylori* (on a glass slide) by free NAMs and DSPE Lpx exposed to gastric mucus isolated from pigs. Note that there was no pre-treatment of the bacteria with ethanol. Negative controls without NAMs (neg) were also included. (a) Representative epifluorescence microscopy images, all taken with the same exposure time. (b) FISH fluorescence normalized to that of free NAMs. Within one experiment, each condition was performed in triplicate. Independent experiments were done using mucus from 3 different pigs. Results are presented as mean values and respective standard deviation.

Discussion

For NAMs to become a novel platform to target infections *in vivo* for diagnosis and therapy, they have to cross biological barriers, like the bacterial cell envelope and the mucus that covers the epithelia, in order to reach their intracellular bacterial targets without loss of activity [23, 72]. We investigated whether liposomes, composed of the cationic lipid DOTAP and the neutral fusogenic lipid DOPE, would be suitable nanocarriers for delivering NAMs across the gastric mucus barrier in *H. pylori* cells. We compared cationic and post-PEGylated lipoplexes, anticipating the need of PEG stabilization to safely cross the harsh gastric environment. Based on previous experiments with mammalian cells, PEGylation typically comes at the price of

reduced cell interactions. Therefore, two different PEGs were tested: DSPE-PEG, which stably incorporates into liposomes, and Cer-PEG, which can diffuse out of the liposomes over time [52, 53].

Before reaching *H. pylori* in the stomach, lipoplexes will encounter the gastric mucus (Figure 1a) which is a tough barrier that limits the diffusion of nanoparticles and molecules [18]. Recently we showed that, while gastric mucus does not hinder the diffusion of the small sized NAMs, binding of mucus components to NAMs does happen which hampers efficient hybridization in *H. pylori* [24]. We reasoned that a nanocarrier that (i) shields NAMs from such interactions and (ii) can penetrate into the mucus where bacteria reside could be valuable [23, 55]. Nanoparticle diffusion through mucus is determined both by their size and surface properties [73]. PEGylation is the commonly employed strategy to limit the adhesive interactions of nanoparticles with mucus [39, 51]. Furthermore, PEGylation may offer additional protection to the NAMs bound at the surface of liposomes by providing a steric barrier against muco-interactions. As the size of the pores in human gastric mucus is still not well characterized [20] we first studied the diffusion of PEGylated nanospheres, varying in size, in mucus isolated from the stomach of pigs. It is of note that porcine gastric mucus is considered to better resemble human mucus than gastric murine or rabbit mucus [57]. Our results suggest that nanoparticles should be smaller than 200 nm to maintain a mobile fraction in gastric mucus (Figure 2a). Although similar diffusion studies in porcine gastric mucus have not yet been performed to our knowledge, our observations are in line with studies in gastrointestinal mucus. For instance in intestinal mucus, using porcine and murine models, it was also reported that PEGylated 500 nm nanospheres were hindered, while PEGylated 200 nm nanospheres were able to penetrate murine small intestinal mucus, but not colonic mucus [20, 74]. This is further supported by the observation that PEGylated 200 and 500 nm nanoparticles distributed

555 throughout the colorectal epithelium of mice *in vivo* less uniformly than PEGylated 100 and 40
556 nm nanospheres [22].
557 Moving on to the diffusion of NAM lipoplexes, we found that PEGylation did improve
558 mobility, although a fraction of the lipoplexes remained immobilized (Figure 2b). This fraction
559 appeared to be higher than for PEGylated nanospheres of similar size (Figure 2a). Although
560 both lipoplexes and nanospheres have a PEGylated surface and thus a substantially reduced
561 surface charge, compared to nanospheres the lipoplexes possess a slightly higher and net
562 positive charge. This may contribute to increased binding, and hence slower diffusion in mucus,
563 as also reported for other cationic nanoparticles in other types of mucus [50, 62, 75].
564 In future work one could consider developing even smaller nanocarriers, such as micelles or
565 self-nanoemulsifying drug delivery systems (SNEDDS) to further improve diffusion in dense
566 gastric mucus [76, 77]. Also, it could be attractive to focus on smaller liposomes which could
567 be prepared by microfluidic mixing [78, 79]. DOTAP-DOPE liposomes of 50 to 75 nm could
568 be reproducibly manufactured in this way [80]. An alternative to enhance diffusion through
569 gastric mucus could be the use of mucolytics. However, the effect of mucolytic agents like N-
570 acetyl-L-cysteine on nanoparticle penetration through mucus is not always clear, while it can
571 irreversibly compromise the functionality of mucus as a defensive barrier against pathogens
572 [76, 81, 82].
573 Next, we evaluated if (PEGylated) Lpx have the potential to deliver NAMs across the cell
574 envelope and into the cytoplasm of *H. pylori* cells. The envelope of gram negative bacteria,
575 composed of a cytoplasmic membrane, periplasm, peptidoglycan layer and an outer membrane
576 [83], is repeatedly reported as a hurdle for oligonucleotide penetration in different bacteria [9,
577 84, 85]. It is believed that oligonucleotides are too large to passively diffuse through the
578 bacterial envelope [8]. The traditional method, therefore, to deliver NAMs in gram negative
579 bacteria *in vitro* involves membrane permeabilization with ethanol [64]. Clearly, ethanol

580 mediated permeabilization is not transferable to *in vivo* conditions which necessitates other
581 methods for the delivery of NAMs into bacterial cells. In this study we evaluated if fusogenic
582 DOTAP-DOPE liposomes could be suitable nanocarriers. As the fluorescent NAMs in the
583 hybridization solution were designed to specifically hybridize in *H. pylori* [49], FISH could be
584 used to evaluate successful intracellular delivery. We found that while the cationic and Cer Lpx
585 hybridization performance was nearly similar to free NAMs in ethanol treated cells, DSPE Lpx
586 performed even markedly better (Figure 3). After removing extracellular membrane bound
587 DSPE Lpx, still a 1-3 fold increase in hybridization efficiency was retained as compared to the
588 standard ethanol protocol (Figure 5). This demonstrates the capacity of DSPE Lpx to
589 successfully deliver NAMs in the cytosol of *H. pylori*.

590 Having found that DSPE Lpx have partial mobility in gastric mucus and can deliver NAMs
591 in the cytosol of *H. pylori*, we finally tested the hybridization efficacy of DSPE Lpx in the
592 presence of gastric mucus. A more than 2 fold improvement in hybridization efficiency was
593 found with DSPE Lpx when compared to free NAMs (Figure 6). This enhancement shows the
594 ability of DSPE Lpx to protect NAMs from interacting with mucus constituents, thus retaining
595 their hybridization activity. We noticed that the remaining adhesion of DSPE Lpx to the
596 bacterial outer membrane, as observed in solution, was almost entirely invisible in the presence
597 of mucus. This may be due to the presence of mucins that compete with lipoplexes for
598 interaction with the bacterial envelope, thereby reducing the sticking of DSPE Lpx to the outer
599 membrane [86, 87]. When the aim is to specifically detect *H. pylori* by FISH in a diagnostic
600 setting, this could be an advantage as it may avoid unspecific fluorescence due to the binding
601 of the DSPE Lpx to non-target bacteria. However, when the aim is to treat the infection, one
602 could argue that reduced interaction with the cell envelope may reduce the delivery efficiency.
603 In that sense active targeting of the lipoplexes towards *H. pylori* membranes, e.g. by conjugation

of mannose-specific or fucose-specific lectins [88, 89], could be evaluated to improve interactions with the bacterial cell envelope and increase the intracellular delivery efficiency.

Based on our encouraging *in vitro* results, future investigation should focus on the *in vivo* performance of DSPE Lpx PS and PO. The necessary dose to diagnose/treat the infection needs to be investigated, considering the potential dose dependent toxicity to the animal. For the diagnosis of the *H. pylori* infection, the *in vivo* detection of the fluorescence signal, its sensitivity and specificity need to be considered. Detection in the stomach could be performed using an existing confocal endomicroscopy probe [90, 91]. Although accessibility may be a limitation, we believe a porcine model would be the indicated *in vivo* model, as it resembles the human gastric environment and mucus barrier much better than mice models [56, 57]. Moreover, it would be feasible for the detection by the endomicroscope probe, as the small size of mice may limit a proper assessment of the endomicroscopy's capability to visualize the fluorescence signal in the animal stomach.

Conclusions

This study shows, for the first time, successful delivery of NAMs into bacterial cells by DSPE-PEGylated liposomes in which also the mucus associated to the bacterial infection is considered as a potential barrier. It shows that such PEGylated liposomes represent a valuable opportunity in the post-antibiotic era to deliver NAMs as a novel class of therapeutic antimicrobials and diagnostic agents. Future research will focus on evaluating DSPE Lpx in other important pathogens, developing smaller carriers to further improve the diffusion of the carriers in mucus and testing their *in vivo* performance.

Acknowledgments

This work was funded by i) POCI-01-0145-FEDER-006939 (Laboratory for Process Engineering, Environment, Biotechnology and Energy – UID/EQU/00511/2013) funded by the European Regional Development Fund (ERDF), through COMPETE2020 - Programa Operacional Competitividade e Internacionalização (POCI) and by national funds, through FCT - Fundação para a Ciência e a Tecnologia, (ii) NORTE□01□0145□FEDER□000005 – LEPABE-2-ECO-INNOVATION, supported by North Portugal Regional Operational Programme (NORTE 2020), under the Portugal 2020 Partnership Agreement, through the European Regional Development Fund (ERDF), iii) DNA mimics Research Project PIC/IC/82815/2007, NORTE-07-0124-FEDER-000022, and iv) PhD fellowship SFRH/BD/84376/2012. The Laboratory of General Biochemistry and Physical Pharmacy, Ghent University is thanked for financial support. This work was performed under the framework of the COST-Action TD1004: Theragnostics for imaging and therapy.

We also thank Jesper Wengel from the Nucleic Acid Center, University of Southern Denmark, for providing the NAMs and Tom Coenye from the Laboratory of Pharmaceutical Microbiology (LPM), Ghent University, for providing the facilities for bacteria manipulation.

References

1. Fonkwo, P.N., Pricing infectious disease: the economic and health implications of infectious diseases. EMBO Reports, (2008). **9**(Suppl 1): p. S13-S17.
2. Zhu, X., Radovic-Moreno, A.F., Wu, J., Langer, R. and Shi, J., Nanomedicine in the management of microbial infection - overview and perspectives. Nano Today, (2014). **9**(4): p. 478-498.
3. Cerqueira, L., Azevedo, N.F., Almeida, C., Jardim, T., Keevil, C.W. and Vieira, M.J., DNA mimics for the rapid identification of microorganisms by fluorescence *in situ* hybridization (FISH). International Journal of Molecular Sciences, (2008). **9**(10): p. 1944-1960.
4. Campbell, M.A. and Wengel, J., Locked vs. unlocked nucleic acids (LNA vs. UNA): contrasting structures work towards common therapeutic goals. Chem Soc Rev, (2011). **40**(12): p. 5680-9.

5. Järver, P., Coursindel, T., Andaloussi, S.E., Godfrey, C., Wood, M.J. and Gait1, M.J., Peptide-mediated cell and *in vivo* delivery of antisense oligonucleotides and siRNA. Molecular Therapy Nucleic acids, (2012). **1**(6): p. 1-17.
6. Ashizawa, A.T. and Cortes, J., Liposomal delivery of nucleic acid-based anticancer therapeutics: BP-100-1.01. Expert Opinion on Drug Delivery, (2015). **12**(7): p. 1107-1120.
7. Good, L., Sandberg, R., Larsson, O., Nielsen, P.E. and Wahlestedt, C., Antisense PNA effects in *Escherichia coli* are limited by the outer-membrane LPS layer. Microbiology, (2000). **146**.
8. Woodford, N. and Wareham, D.W., Tackling antibiotic resistance: a dose of common antisense? J Antimicrob Chemother, (2009). **63**(2): p. 225-9.
9. Mellbye, B.L., Weller, D.D., Hassinger, J.N., Reeves, M.D., Lovejoy, C.E., Iversen, P.L., *et al.*, Cationic phosphorodiamidate morpholino oligomers efficiently prevent growth of *Escherichia coli in vitro* and *in vivo*. J Antimicrob Chemother, (2010). **65**(1): p. 98-106.
10. Laxminarayan, R., Duse, A., Wattal, C., Zaidi, A.K.M., Wertheim, H.F.L., Sumpradit, N., *et al.*, Antibiotic resistance—the need for global solutions. The Lancet Infectious Diseases, (2013). **13**(12): p. 1057-1098.
11. Amann, R. and Fuchs, B.M., Single-cell identification in microbial communities by improved fluorescence *in situ* hybridization techniques. Nat Rev Micro, (2008). **6**(5): p. 339-348.
12. Frickmann, H., Masanta, W.O. and Zautner, A.E., Emerging rapid resistance testing methods for clinical microbiology laboratories and their potential impact on patient management. Biomed Res Int, (2014). **375681**(10): p. 17.
13. Geva-Zatorsky, N., Alvarez, D., Hudak, J.E., Reading, N.C., Erturk-Hasdemir, D., Dasgupta, S., *et al.*, *In vivo* imaging and tracking of host-microbiota interactions via metabolic labeling of gut anaerobic bacteria. Nat Med, (2015). **21**(9): p. 1091-100.
14. Amann, R. and Fuchs, B.M., Single-cell identification in microbial communities by improved fluorescence in situ hybridization techniques. Nat Rev Microbiol, (2008). **6**(5): p. 339-48.
15. Lopes, D., Nunes, C., Martins, M.C., Sarmento, B. and Reis, S., Eradication of *Helicobacter pylori*: Past, present and future. J Control Release, (2014). **189**: p. 169-86.
16. Moussata, D., Goetz, M., Gloeckner, A., Kerner, M., Campbell, B., Hoffman, A., *et al.*, Confocal laser endomicroscopy is a new imaging modality for recognition of intramucosal bacteria in inflammatory bowel disease *in vivo*. Gut, (2011). **60**(1): p. 26-33.
17. Park, P.-G., Cho, M.-H., Rhie, G.-e., Jeong, H., Youn, H. and Hong, K.-J., GFP-tagged *E. coli* shows bacterial distribution in mouse organs: pathogen tracking using fluorescence signal. Clinical and Experimental Vaccine Research, (2012). **1**(1): p. 83-87.
18. Crater, J.S. and Carrier, R.L., Barrier properties of gastrointestinal mucus to nanoparticle transport. Macromol Biosci, (2010). **10**(12): p. 1473-83.
19. Lieleg, O., Vladescu, I. and Ribbeck, K., Characterization of particle translocation through mucin hydrogels. Biophys J, (2010). **98**(9): p. 1782-9.
20. Ensign, L.M., Henning, A., Schneider, C.S., Maisel, K., Wang, Y.Y., Porosoff, M.D., *et al.*, *Ex vivo* characterization of particle transport in mucus secretions coating freshly excised mucosal tissues. Mol Pharm, (2013). **10**(6): p. 2176-82.
21. Wang, Y.Y., Lai, S.K., So, C., Schneider, C., Cone, R. and Hanes, J., Mucoadhesive nanoparticles may disrupt the protective human mucus barrier by altering its microstructure. PLoS ONE, (2011). **6**(6): p. 29.

22. Maisel, K., Ensign, L., Reddy, M., Cone, R. and Hanes, J., Effect of surface chemistry on nanoparticle interaction with gastrointestinal mucus and distribution in the gastrointestinal tract following oral and rectal administration in the mouse. J Control Release, (2015). **197**: p. 48-57.
23. Ribet, D. and Cossart, P., How bacterial pathogens colonize their hosts and invade deeper tissues. Microbes and Infection, (2015). **17**(3): p. 173-183.
24. Santos, R.S., Dakwar, G.R., Xiong, R., Forier, K., Remaut, K., Stremersch, S., *et al.*, Effect of native gastric mucus on *in vivo* hybridization therapies directed at *Helicobacter pylori*. Molecular Therapy. Nucleic Acids, (2015). **4**(12): p. e269.
25. Guo, Q.-Y., Xiao, G., Li, R., Guan, S.-M., Zhu, X.-L. and Wu, J.-Z., Treatment of *Streptococcus mutans* with antisense oligodeoxyribonucleotides to gtfB mRNA inhibits GtfB expression and function. FEMS Microbiology Letters, (2006). **264**(1): p. 8-14.
26. Hou, Z., Meng, J.R., Niu, C., Wang, H.F., Liu, J., Hu, B.Q., *et al.*, Restoration of antibiotic susceptibility in methicillin-resistant Staphylococcus aureus by targeting mecR1 with a phosphorothioate deoxyribozyme. Clin Exp Pharmacol Physiol, (2007). **34**(11): p. 1160-4.
27. Rasmussen, L.C.V., Sperling-Petersen, H.U. and Mortensen, K.K., Hitting bacteria at the heart of the central dogma: sequence-specific inhibition. Microbial Cell Factories, (2007). **6**(1): p. 1-26.
28. Barnes, R.J., Leung, K.T., Schraft, H. and Ulanova, M., Chromosomal gfp labelling of Pseudomonas aeruginosa using a mini-Tn7 transposon: application for studies of bacteria-host interactions. Can J Microbiol, (2008). **54**(1): p. 48-57.
29. Lawson, T.S., Connally, R.E., Iredell, J.R., Vemulpad, S. and Piper, J.A., Detection of Staphylococcus aureus With a Fluorescence In Situ Hybridization That Does Not Require Lysostaphin. Journal of Clinical Laboratory Analysis, (2011). **25**(2): p. 142-147.
30. Readman, J.B., Dickson, G. and Coldham, N.G., Translational Inhibition of CTX-M Extended Spectrum β-Lactamase in Clinical Strains of Escherichia coli by Synthetic Antisense Oligonucleotides Partially Restores Sensitivity to Cefotaxime. Frontiers in Microbiology, (2016). **7**: p. 373.
31. Vaara, M. and Porro, M., Group of peptides that act synergistically with hydrophobic antibiotics against gram-negative enteric bacteria. Antimicrob Agents Chemother, (1996). **40**.
32. Puckett, S.E., Reese, K.A., Mitev, G.M., Mullen, V., Johnson, R.C., Pomraning, K.R., *et al.*, Bacterial resistance to antisense peptide phosphorodiamidate morpholino oligomers. Antimicrobial Agents and Chemotherapy, (2012). **56**(12): p. 6147-6153.
33. Wang, F., Wang, Y., Zhang, X., Zhang, W., Guo, S. and Jin, F., Recent progress of cell-penetrating peptides as new carriers for intracellular cargo delivery. Journal of Controlled Release, (2014). **174**(0): p. 126-136.
34. Young Kim, H., Young Yum, S., Jang, G. and Ahn, D.-R., Discovery of a non-cationic cell penetrating peptide derived from membrane-interacting human proteins and its potential as a protein delivery carrier. Scientific Reports, (2015). **5**: p. 11719.
35. Garza-González, E., Perez-Perez, G.I., Maldonado-Garza, H.J. and Bosques-Padilla, F.J., A review of *Helicobacter pylori* diagnosis, treatment, and methods to detect eradication. World Journal of Gastroenterology : WJG, (2014). **20**(6): p. 1438-1449.
36. Costa, A.M., Leite, M., Seruca, R. and Figueiredo, C., Adherens junctions as targets of microorganisms: a focus on *Helicobacter pylori*. FEBS Lett, (2013). **587**(3): p. 259-65.
37. Li, W. and Szoka, F.C., Lipid-based nanoparticles for nucleic acid delivery. Pharmaceutical Research, (2007). **24**(3): p. 438-449.

38. Forier, K., Raemdonck, K., De Smedt, S.C., Demeester, J., Coenye, T. and Braeckmans, K., Lipid and polymer nanoparticles for drug delivery to bacterial biofilms. Journal of Controlled Release, (2014)(0).
39. Zhang, L., Pornpattananangku, D., Hu, C.M. and Huang, C.M., Development of nanoparticles for antimicrobial drug delivery. Curr Med Chem, (2010). **17**(6): p. 585-94.
40. Gao, W., Thamphiwatana, S., Angsantikul, P. and Zhang, L., Nanoparticle approaches against bacterial infections. Wiley Interdiscip Rev Nanomed Nanobiotechnol, (2014). **6**(6): p. 532-47.
41. Zazo, H., Colino, C.I. and Lanao, J.M., Current applications of nanoparticles in infectious diseases. J Control Release, (2016). **224**: p. 86-102.
42. Meng, J., Wang, H., Hou, Z., Chen, T., Fu, J., Ma, X., *et al.*, Novel anion liposome-encapsulated antisense oligonucleotide restores susceptibility of methicillin-resistant *Staphylococcus aureus* and rescues mice from lethal sepsis by targeting mecA. Antimicrob Agents Chemother, (2009). **53**(7): p. 2871-8.
43. Fillion, P., Desjardins, A., Sayasith, K. and Lagace, J., Encapsulation of DNA in negatively charged liposomes and inhibition of bacterial gene expression with fluid liposome-encapsulated antisense oligonucleotides. Biochim Biophys Acta, (2001). **1515**.
44. Peeters, L., Sanders, N.N., Jones, A., Demeester, J. and De Smedt, S.C., Post-pegylated lipoplexes are promising vehicles for gene delivery in RPE cells. J Control Release, (2007). **121**(3): p. 208-17.
45. Dakwar, G.R., Braeckmans, K., Demeester, J., Ceelen, W., Smedt, S.C.D. and Remaut, K., Disregarded effect of biological fluids in siRNA delivery: human ascites fluid severely restricts cellular uptake of nanoparticles. ACS Applied Materials & Interfaces, (2015). **7**(43): p. 24322-24329.
46. Kim, B.-K., Hwang, G.-B., Seu, Y.-B., Choi, J.-S., Jin, K.S. and Doh, K.-O., DOTAP/DOPE ratio and cell type determine transfection efficiency with DOTAP-liposomes. Biochimica et Biophysica Acta (BBA) - Biomembranes, (2015). **1848**(10, Part A): p. 1996-2001.
47. Nicolosi, D., Scalia, M., Nicolosi, V.M. and Pignatello, R., Encapsulation in fusogenic liposomes broadens the spectrum of action of vancomycin against Gram-negative bacteria. Int J Antimicrob Agents, (2010). **35**(6): p. 553-8.
48. Farhood, H., Serbina, N. and Huang, L., The role of dioleoyl phosphatidylethanolamine in cationic liposome mediated gene transfer. Biochim Biophys Acta, (1995). **1235**(2): p. 289-95.
49. Fontenete, S., Guimarães, N., Leite, M., Figueiredo, C., Wengel, J. and Filipe Azevedo, N., Hybridization-based detection of *Helicobacter pylori* at human body temperature using advanced locked nucleic acid (LNA) probes. PLoS ONE, (2013). **8**(11): p. e81230.
50. Forier, K., Messiaen, A.S., Raemdonck, K., Deschout, H., Rejman, J., De Baets, F., *et al.*, Transport of nanoparticles in cystic fibrosis sputum and bacterial biofilms by single-particle tracking microscopy. Nanomedicine, (2013). **8**(6): p. 935-49.
51. Suk, J.S., Xu, Q., Kim, N., Hanes, J. and Ensign, L.M., PEGylation as a strategy for improving nanoparticle-based drug and gene delivery. Adv Drug Deliv Rev, (2016). **99**(Pt A): p. 28-51.
52. Webb, M.S., Saxon, D., Wong, F.M., Lim, H.J., Wang, Z., Bally, M.B., *et al.*, Comparison of different hydrophobic anchors conjugated to poly(ethylene glycol): effects on the pharmacokinetics of liposomal vincristine. Biochim Biophys Acta, (1998). **1372**(2): p. 272-82.

53. Hu, Q., Shew, C.R., Bally, M.B. and Madden, T.D., Programmable fusogenic vesicles for intracellular delivery of antisense oligodeoxynucleotides: enhanced cellular uptake and biological effects. Biochim Biophys Acta, (2001). **3**(1): p. 1-13.
54. Groo, A.C. and Lagarce, F., Mucus models to evaluate nanomedicines for diffusion. Drug Discov Today, (2014). **19**(8): p. 1097-108.
55. Boegh, M. and Nielsen, H.M., Mucus as a barrier to drug delivery - understanding and mimicking the barrier properties. Basic Clin Pharmacol Toxicol, (2015). **116**(3): p. 179-86.
56. Lai, S.K., Wang, Y.-Y., Wirtz, D. and Hanes, J., Micro- and macrorheology of mucus. Advanced Drug Delivery Reviews, (2009). **61**(2): p. 86-100.
57. Varum, F.J., Veiga, F., Sousa, J.S. and Basit, A.W., Mucus thickness in the gastrointestinal tract of laboratory animals. J Pharm Pharmacol, (2012). **64**(2): p. 218-27.
58. Baele, M., Decostere, A., Vandamme, P., Ceelen, L., Hellemans, A., Mast, J., *et al.*, Isolation and characterization of *Helicobacter suis* sp. nov. from pig stomachs. Int J Syst Evol Microbiol, (2008). **58**(Pt 6): p. 1350-8.
59. Dakwar, G.R., Zagato, E., Delanghe, J., Hobel, S., Aigner, A., Denys, H., *et al.*, Colloidal stability of nano-sized particles in the peritoneal fluid: towards optimizing drug delivery systems for intraperitoneal therapy. Acta Biomaterialia, (2014). **10**(7): p. 2965-2975.
60. Lechanteur, A., Furst, T., Evrard, B., Delvenne, P., Hubert, P. and Piel, G., Development of anti-E6 pegylated lipoplexes for mucosal application in the context of cervical preneoplastic lesions. Int J Pharm, (2015). **483**(1-2): p. 268-77.
61. Forier, K., Messiaen, A.S., Raemdonck, K., Nelis, H., De Smedt, S., Demeester, J., *et al.*, Probing the size limit for nanomedicine penetration into Burkholderia multivorans and Pseudomonas aeruginosa biofilms. J Control Release, (2014). **195**: p. 21-8.
62. Martens, T.F., Vercauteren, D., Forier, K., Deschout, H., Remaut, K., Paesen, R., *et al.*, Measuring the intravitreal mobility of nanomedicines with single-particle tracking microscopy. Nanomedicine, (2013). **8**(12): p. 1955-68.
63. Braeckmans, K., Buyens, K., Bouquet, W., Vervaet, C., Joye, P., Vos, F.D., *et al.*, Sizing nanomatter in biological fluids by fluorescence single particle tracking. Nano Letters, (2010). **10**(11): p. 4435-4442.
64. Fontenete, S., Leite, M., Guimarães, N., Madureira, P., Ferreira, R.M., Figueiredo, C., *et al.*, Towards fluorescence *in vivo* hybridization (FIVH) detection of *H. pylori* in gastric mucosa using advanced LNA probes. PLoS ONE, (2015). **10**(4): p. e0125494.
65. Boegh, M., Baldursdottir, S.G., Mullertz, A. and Nielsen, H.M., Property profiling of biosimilar mucus in a novel mucus-containing *in vitro* model for assessment of intestinal drug absorption. Eur J Pharm Biopharm, (2014). **87**(2): p. 227-35.
66. Dias, N. and Stein, C.A., Antisense Oligonucleotides: Basic Concepts and Mechanisms. Molecular Cancer Therapeutics, (2002). **1**(5): p. 347-355.
67. DiTizio, V., Ferguson, G.W., Mittelman, M.W., Khoury, A.E., Bruce, A.W. and DiCosmo, F., A liposomal hydrogel for the prevention of bacterial adhesion to catheters. Biomaterials, (1998). **19**(20): p. 1877-84.
68. Gon, S., Kumar, K.N., Nusslein, K. and Santore, M.M., How bacteria adhere to brushy PEG surfaces: clinging to flaws and compressing the brush. Macromolecules, (2012). **45**(20): p. 8373-8381.
69. Moss, S.F., Moise, L., Lee, D.S., Kim, W., Zhang, S., Lee, J., *et al.*, HelicoVax: epitope-based therapeutic *Helicobacter pylori* vaccination in a mouse model. Vaccine, (2011). **29**(11): p. 2085-91.

70. Zetterberg, M.M., Reijmar, K., Pranting, M., Engstrom, A., Andersson, D.I. and Edwards, K., PEG-stabilized lipid disks as carriers for amphiphilic antimicrobial peptides. J Control Release, (2011). **156**(3): p. 323-8.
71. Yang, K., Gitter, B., Ruger, R., Albrecht, V., Wieland, G.D. and Fahr, A., Wheat germ agglutinin modified liposomes for the photodynamic inactivation of bacteria. Photochem Photobiol, (2012). **88**(3): p. 548-56.
72. Kole, R., Krainer, A.R. and Altman, S., RNA therapeutics: beyond RNA interference and antisense oligonucleotides. Nat Rev Drug Discov, (2012). **11**(2): p. 125-40.
73. Wang, Y.Y., Lai, S.K., Suk, J.S., Pace, A., Cone, R. and Hanes, J., Addressing the PEG mucoadhesivity paradox to engineer nanoparticles that "slip" through the human mucus barrier. Angew Chem Int Ed Engl, (2008). **47**(50): p. 9726-9.
74. Yildiz, H.M., McKelvey, C.A., Marsac, P.J. and Carrier, R.L., Size selectivity of intestinal mucus to diffusing particulates is dependent on surface chemistry and exposure to lipids. J Drug Target, (2015). **23**(7-8): p. 768-74.
75. Abdulkarim, M., Agullo, N., Cattoz, B., Griffiths, P., Bernkop-Schnurch, A., Borros, S.G., *et al.*, Nanoparticle diffusion within intestinal mucus: Three-dimensional response analysis dissecting the impact of particle surface charge, size and heterogeneity across polyelectrolyte, pegylated and viral particles. Eur J Pharm Biopharm, (2015). **97**(Pt A): p. 230-8.
76. Dünnhaupt, S., Kammona, O., Waldner, C., Kiparissides, C. and Bernkop-Schnürch, A., Nano-carrier systems: Strategies to overcome the mucus gel barrier. European Journal of Pharmaceutics and Biopharmaceutics, (2015). **96**: p. 447-453.
77. Jeong, J.H., Kim, S.H. and Park, T.G., Targeted antisense oligonucleotide micellar delivery systems, in *Nanotechnology for Cancer Therapy*, M.M. Amiji, Editor. (2007), CRC Press: Florida.
78. Belliveau, N.M., Huft, J., Lin, P.J.C., Chen, S., Leung, A.K.K., Leaver, T.J., *et al.*, Microfluidic synthesis of highly potent limit-size lipid nanoparticles for *in vivo* delivery of siRNA. Molecular Therapy. Nucleic Acids, (2012). **1**(8): p. e37.
79. Zhigaltsev, I.V., Belliveau, N., Hafez, I., Leung, A.K.K., Huft, J., Hansen, C., *et al.*, Bottom-up design and synthesis of limit size lipid nanoparticle systems with aqueous and triglyceride cores using millisecond microfluidic mixing. Langmuir, (2012). **28**(7): p. 3633-3640.
80. Kastner, E., Verma, V., Lowry, D. and Perrie, Y., Microfluidic-controlled manufacture of liposomes for the solubilisation of a poorly water soluble drug. Int J Pharm, (2015). **485**(1-2): p. 122-30.
81. Ensign, L.M., Cone, R. and Hanes, J., Oral drug delivery with polymeric nanoparticles: the gastrointestinal mucus barriers. Advanced Drug Delivery Reviews, (2012). **64**(6): p. 557-570.
82. Sigurdsson, H.H., Kirch, J. and Lehr, C.-M., Mucus as a barrier to lipophilic drugs. International Journal of Pharmaceutics, (2013). **453**(1): p. 56-64.
83. Moran, A.P., Microbial glycobiology., in *Structures, relevance and applications* A.P. Moran, et al., Editors. (2009), Elsevier: London.
84. Eriksson, M., Nielsen, P.E. and Good, L., Cell permeabilization and uptake of antisense peptide-peptide nucleic acid (PNA) into *Escherichia coli*. J Biol Chem, (2002). **277**.
85. Nekhotiaeva, N., Awasthi, S.K., Nielsen, P.E. and Good, L., Inhibition of *Staphylococcus aureus* gene expression and growth using antisense peptide nucleic acids. Mol Ther, (2004). **10**.
86. Joosten, M., Lindén, S., Rossi, M., Tay, A.C.Y., Skoog, E., Padra, M., *et al.*, Divergence between the highly virulent zoonotic pathogen *Helicobacter heilmannii* and Its closest

relative, the low-virulence "*Helicobacter ailurogastricus*" sp. nov. Infection and Immunity, (2016). **84**(1): p. 293-306.
87. Testerman, T.L., McGee, D.J. and Mobley, H.L.T., Adherence and Colonization, in *Helicobacter pylori: Physiology and Genetics*, H.L.T. Mobley, G.L. Mendz, and S.L. Hazell, Editors. (2001), ASM Press: Washington (DC).
88. Gao, W., Thamphiwatana, S., Angsantikul, P. and Zhang, L., Nanoparticle approaches against bacterial infections. Wiley interdisciplinary reviews. Nanomedicine and nanobiotechnology, (2014). **6**(6): p. 532-547.
89. Umamaheshwari, R.B. and Jain, N.K., Receptor mediated targeting of lectin conjugated gliadin nanoparticles in the treatment of *Helicobacter pylori.* J Drug Target, (2003). **11**(7): p. 415-23.
90. Neumann, H., Gunther, C., Vieth, M., Grauer, M., Wittkopf, N., Mudter, J., *et al.*, Confocal laser endomicroscopy for in vivo diagnosis of Clostridium difficile associated colitis - a pilot study. PLoS One, (2013). **8**(3): p. e58753.
91. Nonaka, K., Ohata, K., Ban, S., Ichihara, S., Takasugi, R., Minato, Y., *et al.*, Histopathological confirmation of similar intramucosal distribution of fluorescein in both intravenous administration and local mucosal application for probe-based confocal laser endomicroscopy of the normal stomach. World Journal of Clinical Cases, (2015). **3**(12): p. 993-999.